Autonomous Vision-based Unmanned Aerial Spray System with Variable Flow for Agricultural Application

Manuel Chad Agurob, Amiel Jhon Bano, Immanuel Paradela, Steve Clar, Earl Ryan Aleluya,
Carl John Salaan, *Member, IAENG*

Abstract— **The study focuses on implementing an independent aerial sprayer system with vision sensors for autonomous agrochemical applications using advances in precision agriculture. Poor planting management often leads to unpredictable vegetation vigor in croplands, resulting in wasted agrochemical inputs. Achieving precise spraying flow control using typical UAVs over crop fields is challenging. This study's aerial sprayer system can evaluate crop health using a visual-based RGBVI calculation, made possible by incorporating an RGB camera and a small computer. The system measures VIs, determines plant health, and controls the input flow rate. The autonomous vision-based aerial spraying system responds by detecting the real-time interpretation of the Red Green Blue Vegetation Index (RGBVI) for low and high vegetation vigor. It regulates the flow rate by generating a square pulse wave with varying duty cycles. The system uses an 850 mm hexacopter with a 3-kg liquid solution tank that can spray up to 800 ml/min, establishing a direct relationship between varying RGBVI and the duty cycle. When the duty cycle is between 50% and 100%, nozzle flow ranges from 2.85 mL to 5.78 mL per 30 seconds. A comparison was made on the planned flight routes and trajectories flown to assess the drone's autonomous flight capabilities in following the terrain. The drone sprayer could follow its intended path autonomously with an average deviation of 6.72cm and a terrain-following error of only 0.2%.**

Keywords—*Vision-based sprayer system, Aerial Sprayer System, Agricultural drone, Vegetation Index*

I. INTRODUCTION

MAJOR crops, which include fruit crops, industrial crops, vegetables, and root crops, account for more than 60 percent of total crop production in the Philippines. Crops accounted for 54.9 percent of total production value in agriculture and fisheries, with a 2.8 percent decline in the second quarter of 2022 [1].

M.C. Agurob is a graduate student of the Department of Mechanical Engineering and Technology at Mindanao State University – Iligan Institute of Technology, Iligan City, Philippines (e-mail: manuelchad.agurob@g.msuiit.edu.ph).

A. J. Bano is a researcher at Mindanao State University – Iligan Institute of Technology, Iligan City, Philippines (e-mail: amieljhon.bano@g.msuiit.edu.ph).

I. Paradela is a researcher at Mindanao State University – Iligan Institute of Technology, Iligan City, Philippines (e-mail: Immanuel.paradela@g.msuiit.edu.ph).

S. Clar is a researcher at Mindanao State University – Iligan Institute of Technology, Iligan City, Philippines (e-mail: immanuel.paradela@g.msuiit.edu.ph).

E.R. Aleluya is an assistant professor of the Department of Electrical Engineering and Technology, Mindanao State University – Iligan Institute of Technology, Iligan City, Philippines (e-mail: earlryan.aleluya@g.msuiit.edu.ph).

C. J. Salaan is a professor of the Department of Electrical Engineering and Technology Mindanao State University – Iligan Institute of Technology, Iligan City, Philippines (e-mail: carljohn.salaan@g.msuiit.edu.ph).

Fig. 1. Vision-based unmanned aerial system sprays at a variable rate over a vegetable field

Modern crop cultivation methods in the Philippines have led to a steady increase in harvest. Produce farming has transformed from low-input agriculture using traditional methods and varieties to modern high-input farming using agricultural inputs such as inorganic fertilizers, herbicides, and irrigation to boost crop yield [2]. However, the absence of nutrients ultimately impacts crop growth and profit. This nutritional deficit may result from various environmental variables, including weather, soil conditions, and nutrient availability. One practical approach for increasing crop output is supplying plants with foliar fertilizer sprayed directly onto the leaves rather than the soil. Liquid fertilizer directly administered to leaves has improved fresh matter, leaf area index, and plant height [3]. Figure 1 depicts the mission flight of a vision-based unmanned aerial spraying system as it hovers over a vegetable field at a variable rate generated independently by each micro-motor pump.

Several recent reports have investigated the use of unmanned aerial vehicles (UAVs) for agriculture crop spraying and fertilizer assessment. UAVs for remote sensing may provide information on agricultural crop production systems and detect quantifiable leaf blight across broad regions [4].

Figure 2 illustrates the use of drones for remote monitoring of corn health [5]. The picture overlays boxes to identify specific areas needing more nutrients. These areas would show low vegetative vigor during early stages in the crop's growth, as indicated by the vegetation index. Poor management during the planting stage can lead to random

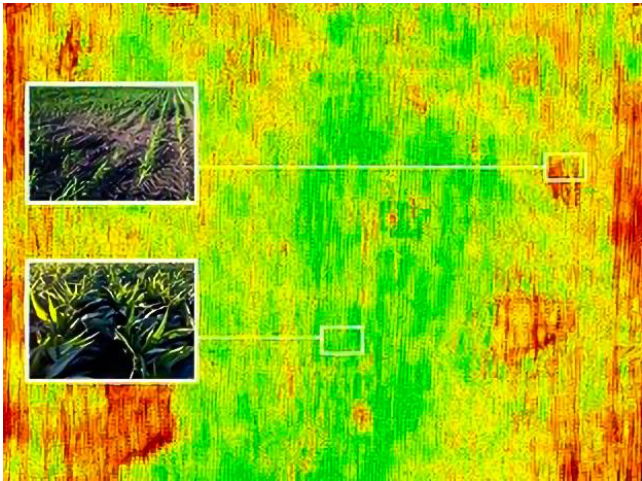plant growth in croplands, resulting in wasted agrochemical inputs.

Fig. 2: Remote assessment of corn health as one of many applications of drones to agriculture.

The Normalized Difference Vegetation Index (NDVI) is the most widely used indicator of vegetation health [6]. It quantitatively measures greenness and overall plant health by comparing near-infrared and visible red reflectance, indicating photosynthetic activity and biomass accumulation. Passive sensors are typically utilized in the remote sensing of vegetation to gather information regarding the electromagnetic wave reflectance produced by canopies, depending on the type of plant, the amount of water inside the tissues, and various other intrinsic characteristics [7]. The chemical and morphological characteristics of the surface of plant organs or leaves determine vegetation's reflectance onto the electromagnetic spectrum [8]. Reflecting near-infrared light into the surrounding environment is a characteristic of healthy plant leaves while reducing chlorophyll production results in a lower quantity of reflected near-infrared light [9]. This technique can evaluate a crop's overall health by comparing the intensities of reflected visible and near-infrared light using the NDVI method. UAV-based RGB pictures can determine the potential of plant cover and VIs to indicate Leaf Nutrient Content (LNC) in corn and predict crop nitrogen use efficiency [10]. Attaching sensors to UAV platforms allows various indices for analyzing plant stress loads to be computed, allowing for real-time, non-destructive agricultural monitoring. Equipped with sensors, UAVs can detect uneven plant growth and identify issues resulting from variable planting, improper seeding, or excessive fertilizing. These actions can lead to irregular crop growth [11], contributing to plant development's inconsistency.

UAVs used as remote sensing to monitor plant health will enable the farmer to make educated decisions, particularly regarding the large size of the rice field and the required number of foliar fertilizers or pesticide applications. The number of treatments necessary depends upon the crop's growth uniformity throughout the area. Farmers manually operate plant protection spraying equipment on the ground to tackle this issue. However, these ground-based conventional sprayers are hindered by several problems,

such as topography and later phases of crop growth. The farmer's field performance regarding adaptability and operations is insufficient [12].

On the other hand, unmanned aerial vehicles (UAVs) provide cheaper costs, simple deployment, near-real-time imagery for visual inspection, less rivalry for photos, and the potential to circumvent weather constraints, particularly cloud cover. Arguably practical applications of drone technology include forest health monitoring, fire mapping applications, forest inventory, wildlife surveys, avalanche patrols, air quality monitoring, plume tracking, groundwater discharge monitoring, and precision agriculture for monitoring crop health [13]. Agricultural drones will play a significant role in precision agriculture, delivering advantages such as fast field measurements, crop and soil condition monitoring, seed planting, fertilizer and pesticide application, irrigation, and farm surveillance. The Department of Agriculture of the Philippines conducted several experiments for years, and the findings demonstrated that the technique could considerably boost food output. In response, the agency is currently issuing directives and vigorously promoting the use of drones [14].

Across several countries, pesticide and fertilizer application by drones is already widespread. Drone sprayers can even reach steep corners at high altitudes, such as those seen in various crop fields, minimizing the labor the farmers require. Spraying drones can access relatively tight areas, enhancing productivity and lowering expenses. The UAV drone sprayer has the potential benefit compared to backpack spraying. It reduces the exposure of the applicator, improves application quality in hard-to-reach places, and makes precise zone or spot application easier when used with UAV-based plant health scouting [15], [16]. The current drone sprayer has environmental concerns regarding assessing off-target spray drift, target deposition, and rotor turbulent air effect. The release height of the application; the position of the nozzle with the rotors; understanding the turbulent airflow from multi-rotors and the potential interaction of any downdraft from the rotors with the canopy or ground; and the effect of UAV sprayer system design, height, and forward speed on the potential for downdraft are some of the unique risks [17]. MG-1 and V6A commercial drone sprayers have provided remote aerial applicators with recommendations about the optimal application height and ground speed for their remotely piloted aerial application systems (RPAAS) to apply pest control products [18] effectively. It is observed that a standard UAV spraying system is designed to operate and allow each nozzle to deliver the same volume of liquid. Because of this, a uniform application of fertilizer or pesticides in areas with vacant patches and uneven growth of crops may be complex. The use of commercial drones in vital services such as fighting forest fires [19], [20], conducting searches and rescues [21], inspecting infrastructure [22], and delivering packages [23] is becoming increasingly common. These drone applications have an exact navigation system (GPS), a camera, and an audio interface. These critical drone applications come with a global positioning system (GPS), a camera, and an audio input/output interface [24]. The precise location of the UAV can either be controlled automatically by the onboard computers or remotely by a pilot at the Ground Control Station (GCS). The ground

control station application is responsible for maintaining the movement of a UAV by transmitting waypoints and other commands to the UAV, as well as monitoring the data received from the UAV. Acquiring an absolute position by utilizing GPS is essential in applications of a drone flying in the air because it provides the performance necessary for autonomous flight [25], [26].

In contrast, others use the historical visiting points in flight as virtual landmarks to correct the positioning result of UAVs [27]. With the advent of computer vision for studies related to the development of autonomous systems [28], applying a vision sensor system to a UAV spraying system will identify site-specific areas and control the required amount of fertilizer or pesticides in that area. Additionally, agriculture sprayers operated through unmanned aerial vehicles (UAVs) have been the research subject due to their significant cost savings and risk effectiveness compared to conventional spraying methods and human-crewed aircraft [29].

This study proposes developing an autonomous vision-based UAV robotic spraying system capable of measuring VIs, determining plant health conditions, and controlling the appropriate input flow rate. By carrying a spectral camera and a small computer, the vision-based aerial spray system can assess the RGBVI of valued crops. This system, which measures the RGBVI, accurately identifies low and high vegetation vigor, enabling precise agrochemical applications. The processed vegetation index will aid the decision-making of the two separate motor pumps through the small single-board computer. Consequently, a variable flow rate will regulate the quantity of liquid fertilizer or pesticides in areas detected by the real-time vision sensor. To maintain control over the spraying system, users must pay attention to the spraying method, the spraying pattern, and the variable control of the sprayer. Equipping a UAV spraying system with vision-based drone sprayer systems with varying flow rates based on the crop's vegetation index can significantly boost crop yield. Compared to conventional agricultural sprayers, automated processes combining remote sensing of plant health with variable rates can potentially increase work efficiency.

II. AUTONOMOUS AERIAL SPRAY SYSTEM CONCEPT AND DESIGN

A. General Concept

Estimating agricultural characteristics, such as chlorophyll and nitrogen content, plant height, above-ground biomass, yield, and fractional vegetation cover, are a few applications widely used for unmanned aerial vehicles (UAVs) in agriculture. Compared to satellite remote sensing, the low cost, portability, high spatial resolution, and high temporal resolution of UAVs have made these estimations possible [30]. Figure 3 illustrates the general concept of aerial spray systems. The drone, equipped with a sprayer system, flies over corn crops and captures crop images, as shown in Fig. 3 (a). The raw image is processed and controlled on the small onboard computer, as in Fig. 3 (b).
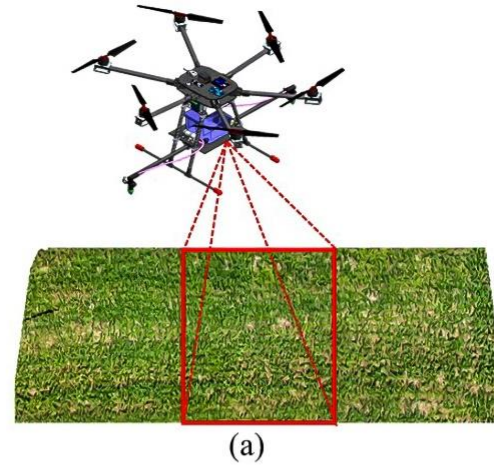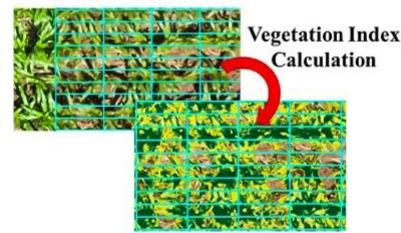
Fig. 3. General concept of vision-based aerial spray system with variable flow starting from (a) taking real-time video, (b) image processing, and (c) vision-based variable-rate spraying.

In Figure 3, an illustration shows a sprayer-equipped drone hovering over a crop field to capture photos (a). The RGBVI method calculates the image's vegetation index (b), which is then transformed into a specific volume flow and subsequently to the duty cycle. The controller activates the two pumps and varies the flow through the pump driver, as depicted in Fig. 3 (c). This process is looped continuously at specific time intervals. The automatic and variable control allows the sprayers to deposit independently with varying flow rates depending on the plant's health status. This method allows for efficient consumption of spray material, such as pesticides, as it is spread according to the severity of the plant's health.

B. The Hardware Setup

The autonomous hardware configurations of the vision-based unmanned aerial spray system are shown in Figure 4. This design implements the autonomous flight mission with two primary elements: an onboard full carbon fiber airframe hexacopter and a ground control system. The 850mm airframe consists of two hardware components: the sprayer system mechanism and the essential connections of the flight controller. The electrical contacts of the components, including propulsion, sensor, communication, and sensor, are also displayed on the flight controller board. An isolated LiPo battery is also used to operate the micro-motor pumps to avoid noise integration into the control and communication system.
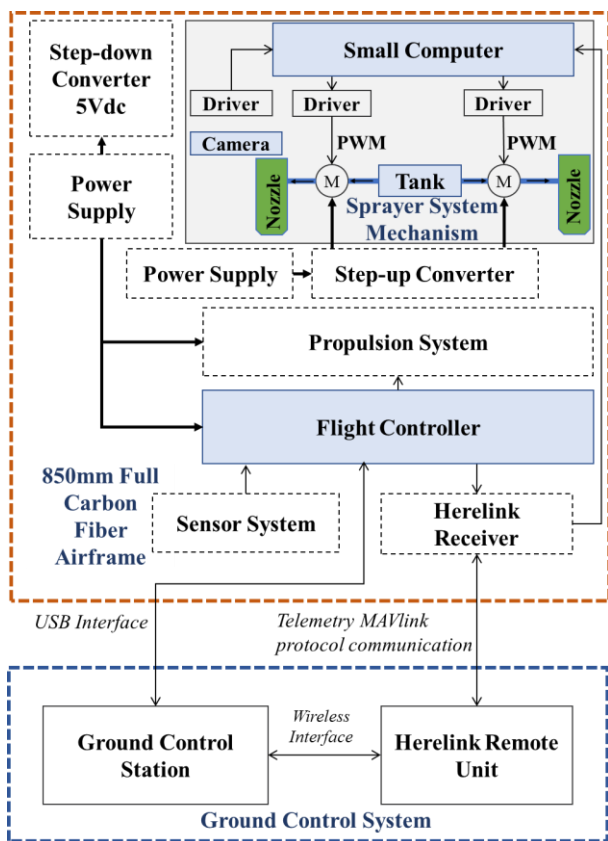

Fig. 4. Configuration of an autonomous vision-based unmanned aerial variable flow spray system

The airframe structure includes upper and lower plates positioned at the center to allocate the assembly of the flight controller, sensor, communication devices, step-up and step-down converters, and batteries. The leg frames hold the plate where the tank, motor pumps, spray boom, spray hose-nozzle assembly, and GoPro camera are installed. The six arms support the propulsion system, comprising six Brushless DC motors (BLDC), six Electronic Speed Controllers (ESC), and six fiber propellers.

C. Design of Sprayer Mechanism

Figure 5 illustrates the computer-aided design (CAD) model of the spraying system attached to the drone.

Various characteristics, such as weight capacity and size, were considered to ensure the drone could carry and accommodate the entire spray system. The CAD model was evaluated based on how well each part of the spraying system would fit on board with minimal interference from other components or the surrounding environment. Fitting all necessary equipment ensured all details remained intact while maximizing crop protection and pest control application efficiency.

Fig. 5 CAD model of the aerial sprayer system as designed in this study

The researchers utilized a hexacopter with ample space and the capability to carry a substantial amount of weight for delivering the various components of the sprayer system, as illustrated in Figure 6. The autonomous drone sprayer comprises a liquid tank, a micro-motor pump, a sprayer boom, tubes, and spray nozzles. Additional elements such as a camera and minicomputer are necessary for image processing and control.
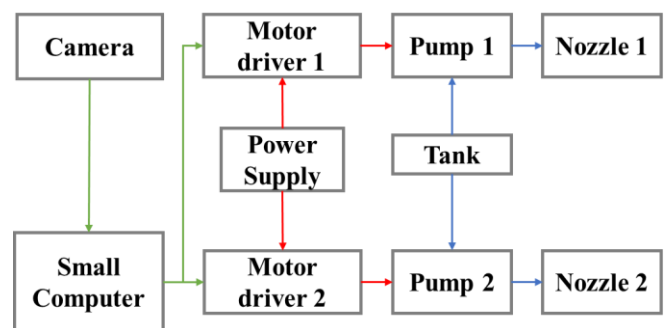

Fig. 6. The component block diagram of the proposed aerial spray system.

Two adjacent nozzles are positioned on the frontal plane of the drone to operate the system. The spray bandwidth, S, represents the expected flow direction and span produced by the flat fan spray-type nozzle, and D represents the distance between the two nozzles. Ø and h represent spray angle and elevation, as shown in Figure 7.

The researchers conducted a UAV flight campaign at midday to collect the necessary data for constructing

RGB-based vegetation indices. These images were further processed using specialized software that generated vegetation indices based on the red, green, and blue (RGB) bands. This information is essential for monitoring changes in plant health over time or assessing environmental conditions in any region. The vision-based hexacopter sprayer system was equipped with a GoPro camera with a resolution of 4K and was oriented perpendicular to the ground. Images were captured by following the land's contours approximately one meter above the ground. The images were taken using a constant aperture and white balance for consistency.
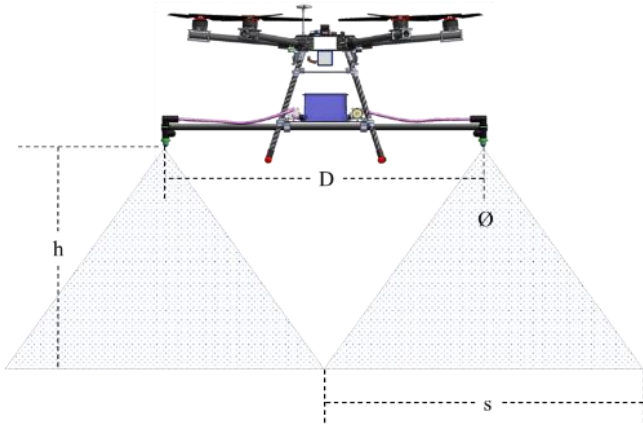

Fig. 7. The CAD model above illustrates the spray flow direction and span.

D. Spray Control System

Figure 8 shows two systems used in autonomous vision-based UAV sprayers with variable flow rates in precision agriculture to monitor and control plant growth. System A converts RGB crop images to vegetation index using image processing. Agriculture uses the vegetation index to monitor plant growth and health. Calculating the vegetation index involves analyzing RGB images captured by a camera or drone and utilizing the reflectance values of the red, green, and blue electromagnetic spectrum.

The second system receives the vegetation index from the first system. It operates using a feed-forward open-loop system, as shown in Fig. 8b. The variable flow rate sprays the plant based on the vegetation index received from the first system. The second system is designed to enable foliar fertilizer application based on the vegetation index received from the first system. It consists of a controller, PWM signal generator, motor driver, micro-motor pump, and sprayer nozzles that allow for variable flow rate sprays dependent on individual plant requirements.

The motor driver amplifies and conditions the PWM signal to precisely control the micro-motor pump's liquid flow rate. Its duty cycle controls this output precisely to ensure optimal growth conditions.
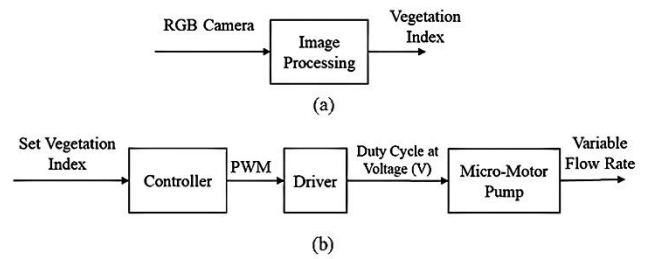

Fig. 8: Two separate functional block diagrams: (A) System converting RGB captured images to Vegetation Index (B) Feed-forward open-loop system from Vegetation Index to Flow Rate

The RGB to vegetation index conversion system and the feed-forward open-loop system work together to accurately monitor and control the volume of agrochemicals applied to plants. The RGB system provides input data for the open loop, which then adjusts the flow rate accordingly to maintain a desired level of chemical application. This combination ensures that precise amounts are administered, efficiently using resources while maximizing plant health benefits. The vegetation index is an essential measure of the health and greenness of local vegetation, which can be determined using remote sensing techniques such as satellite imagery or drones. The UAV sprayer system's connected cameras take RGB pictures that are then processed to determine the vegetation index. The proposed system incorporates a proportional-integral-derivative (PID) controller with a Kp gain factor to produce a digital pulse width modulation (PWM) signal from the input of the first system. The digital signal consists of duty cycles varying in pulse widths and frequencies, providing precise control over the vegetation levels. The PWM signal is then transmitted to the motor driver for conditioning, amplification, and voltage conversion before being applied to control the motion of the motors, as shown in Figure 9. Accurately manipulating these parameters makes it possible to attain an optimal vegetation level while ensuring efficient system operation.
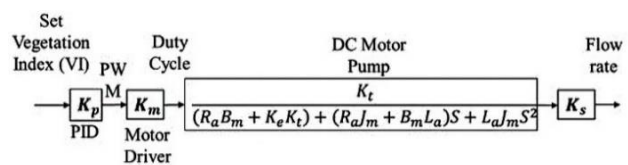
Fig. 9: A schematic of the UAV sprayer control system's varying flow rate

The micro-motor pump receives a voltage signal from the motor driver and modifies the signal's duty cycle to regulate the flow rate of the liquid. A desired duty cycle equation calculates the duty cycle from an inputted voltage, resulting in a variable flow rate that reflects the amount of liquid flowing. The flow rate is affected by the micro-motor pump's characteristics and the voltage signal's duty cycle, represented by a constant gain Ks derived from equation 1.

$$\frac{F(s)}{D(s)} = \frac{K_t}{(R_aB_m+K_eK_t)+(R_aJ_m+B_mL_a)S+(L_aJ_m)S^2} \quad (1)$$

Required parameters:

Maximum speed: $\omega, \frac{rad}{s}$.

Armature current: A_{max}, A

Rotor Inertia: $J_m, \frac{N-m-s^2}{rad}$

Vicious Friction: $B_m, \frac{N-m-s}{rad}$

Voltage Constant: $K_e, \frac{V-s}{rad}$

Torque Constant: $K_t, \frac{N-m}{A}$

Terminal Resistance: $R_a, \Omega \ (Ohms)$

Terminal Inductance: $L_a, H \ (Henry$

The open-loop system maintains desired levels of sprayer volume and required deposits for vegetation growth by adjusting the liquid flow rate based on a vegetation index input. The stability and performance of the system can be verified by testing and analyzing the results using the Routh-Hurwitz stability analysis.

E. The Characterization of the Applied Vegetation Index

Properly characterizing RGBVI data is vital to assess vegetation accurately. This characterization involves understanding the connection between vegetation indices and the lighting conditions under which the data is collected. When characterizing plant RGBVI values, it is necessary to analyze the distribution of RGBVI values for different vegetation types, evaluate the relationship between the RGBVI values and the sun's angle during data collection, and comprehend the impact of atmospheric conditions on RGBVI values. These factors can significantly impact the accuracy of the RGBVI data and must be considered during the analysis. Therefore, understanding the various environmental factors that can influence RGBVI values is crucial for ensuring that the data is correctly interpreted and used for optimal results. Consistent lighting conditions can provide appropriate light intensity and stability for digital photo capture, making it convenient for data analysis to use digital images [31]. However, variations in sunlight strength can result in varied image appearances in different lighting conditions [32]. Advancements in color image acquisition have led to color-based vegetation indices (VIs) derived from digital color cameras being extensively used in assessing crop physiological features. UAVs have become an invaluable tool in agricultural applications due to their low cost, portability, and high spatial and temporal resolutions. UAVs can estimate various crop traits such as chlorophyll content, nitrogen content, plant height, above-ground biomass yield, and fractional vegetation cover. Table I shows that the vegetation indices are based on the

red, green, and blue (RGB) color system. These characteristics include aspects of the leaf's texture and shape in addition to its nitrogen and chlorophyll contents and the shape of the leaf itself [34]–[37]

TABLE I
VEGETATION INDICES BASED ON "GREENNESS"

Vegetation Index	Equation	Reference
Green Leaf Index (GLI)	$\dfrac{2G - R - B}{2G + R + B}$	[38]
Kawashima Index	$R - B$	[33]
Excess Green (ExG) Index	$2G - R - B$	[39]
Green Red Vegetation Index (GRVI)	$\dfrac{G - R}{G + R}$	[40]

Collecting RGB imagery through UAV is a direct and economical method. RGBVI [41] can be calculated from the imagery shown in Equation 1, which is the vegetation index used in this study. UAV-based RGB photography enables retrieval of RGBVI and plant height information from the same dataset during crop monitoring. Combining both metrics provides a more accurate biomass estimate according to RGBVI.

F. Vision System and Variable Flow Spray Strategy

Figure 10 illustrates the process flow of the vision system, which is essential for its operation. The camera takes a picture and transmits it to the onboard computer for further processing. This step is critical as it allows the computer to analyze and interpret what has been captured by the camera. Without this crucial link between capturing an image and sending it to be processed, the vision system would not function. Therefore, taking pictures with a camera plays an integral role in enabling accurate analysis of images by computers within such systems. Afterward, the average values of the pixels are taken to get the two-by-three (2x3) size for RGB, and a 2D matrix of RGB values is created. The study used the RGB Vegetation Index (RGBVI) as a simple way to use the vegetation index. Equation 1 determines the Vegetation Index of the RGB values.

The small computer then transforms the RGBVI values into the desired percentage-equivalent ratio and stores it in a matrix. Once this process is complete, the RGBVI matrix is converted into a string, generating a pulse width modulation (PWM) duty cycle. The real-time vision sensor reads the RGBVI and sprays a controlled quantity of liquid fertilizer or pesticides based on the detected vegetation index. As the sprayer's flow relies on the vegetation index provided by the vision system, the controller automatically adjusts the volume of fertilizer or pesticides deposited per cycle based on Equation 2, ensuring that the correct amount is applied for optimal results. If the RGBVI value gets close to 1.0, indicating the plant is healthy, the system will spray the least amount possible.

```
┌──────────────┐
│    Start     │
└──────────────┘
        │
        ▼
┌──────────────────────┐
│ Camera capture       │
│ pictures and send    │
│ frames to Raspberry  │
│ Pi                   │
└──────────────────────┘
        │
        ▼
┌──────────────────────┐
│ Average the pixel    │
│ value of each frames │
│ into desired         │
│ dimension of BGR and │
│ Calculate RGB        │
│ Vegetation Index     │
│ (RGBVI)              │
└──────────────────────┘
        │
        ▼
┌──────────────────────┐
│ Convert 2D matrix in │
│ 1D matrix and        │
│ extract RGBVI values │
│ from indices 2 and 3 │
└──────────────────────┘
        │
        ▼
┌──────────────────────┐
│ Composed RGBVI       │
│ message by           │
│ converting RGBVII    │
│ matrix values into   │
│ string with timecode │
└──────────────────────┘
        │
        ▼
┌──────────────────────┐
│                      │
│   PWM Duty Cycle     │
│                      │
└──────────────────────┘
        │
        ▼
┌──────────────┐
│     End      │
└──────────────┘
```
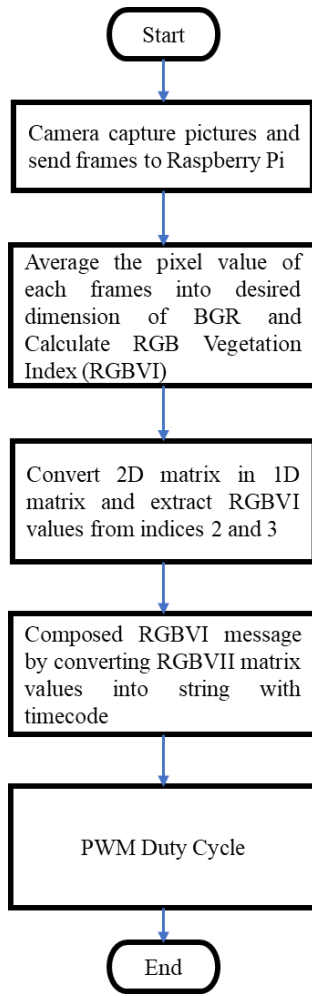
Fig. 10. The step-by-step vision system process flow from real-time video capture, image processing, VI calculations, and PWM cycle generation

$$RGBVI = \left[\frac{(Green \times Green) - (Red \times Blue)}{(Green \times Green) + (Red \times Blue)}\right] \quad (2)$$

On the other hand, if the RGBVI value is approaching 0.0, indicating that the plant is in poor health, the system will spray the maximum volume. The flow rate equation can be adjusted depending on the amount of spray required and the vegetation index. The system uses pulse width modulation (PWM), which involves effectively chopping the power and switching between the supply and the motor at a predetermined rate to take control of the spray deposit.

G. Testing and Calibration Procedure

The image processing component will be tested to calculate the RGBVI using three colors ranging from brown to green, reflecting unhealthy to healthy crop conditions. Consideration must be given to the actual spray and its bandwidth relative to height for analyzing the sprayer mechanism configuration. The RGBVI index values are expected to range from 0.0 to 1.0, with the sample for analysis including soil with a trace of grass and light and dark green grass. Considering these factors is essential for determining an appropriate distance between two nozzles and finding a suitable spray height to achieve a minimal gap when varying duty cycle values of both nozzles during calibration tests. These tests ensure identical flow rates before testing the aerial spraying system during a flight. Furthermore, it validates our findings on optimal performance parameters for efficient use of resources while ensuring adequate application coverage even at low altitudes or in windy conditions, if any arise during operation.

H. Autonomous Mission Planning

The autonomous flight system will be tested in an open area in Iligan City, Philippines, on Mindanao Island. As shown in Figure 11, the waypoints cover an area of 100 square meters, with the starting point at an elevation of approximately 20.23 meters above sea level. The take-off point's latitude and longitude are 8.2495565 and 124.2506241, respectively. The drone sprayer will maintain a height of 5 meters along the path, with only 1 meter separating each of the 22 waypoints. A LiDAR sensor will monitor the drone's altitude above the ground and follow the terrain contours, allowing it to adjust its flight path accordingly. Another drone will fly over the entire waypoint zone, hovering slightly above it to record the sprayer system's flight path
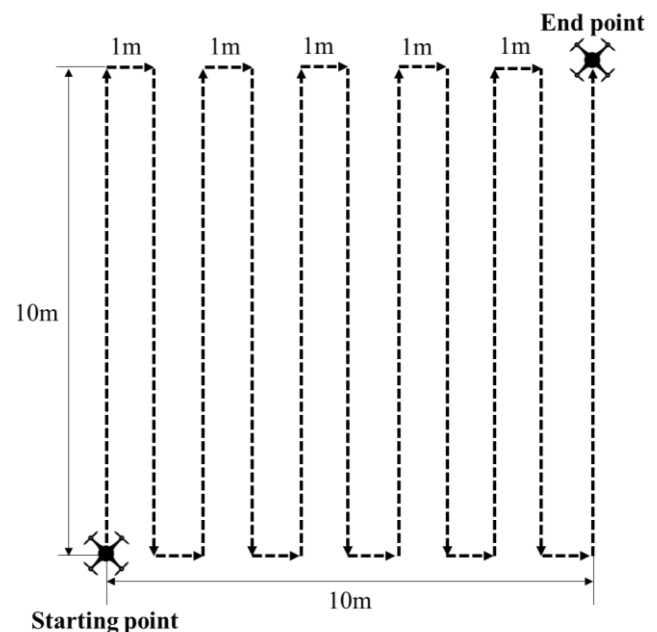
Fig. 11. The UAV sprayer path plan at a 1-meter line interval over a 10x10m area

The sprayer system's flight path was precisely recorded using a second drone to fly over the entire waypoint zone and hover slightly above it, providing an invaluable tool for monitoring its exact trajectory. This method ensured that all areas were covered promptly, with minimal error. Using two

drones, the researchers captured detailed footage from both perspectives, ensuring no area was left untreated or overspray. The waypoints for drone sprayers conducting surveys are pinpointed manually using RTK GPS. The ground control station application monitors the data received from an unmanned aerial vehicle (UAV) and controls its movement by providing waypoints and other commands. The Mission Planner software interfaces with Google Maps, providing a point-and-click interface for selecting waypoints. This mission documentation gives the pilot a straightforward technique for plotting a path for the UAV to follow.

III.   RESULTS AND DISCUSSIONS

A. The Developed Vision-Based Unmanned Aerial Sprayer System

Figure 12 shows the developed aerial spray system. The system utilized an 850-mm hexacopter with a 16-inch propeller and 320-KV brushless motor as an aerial platform.
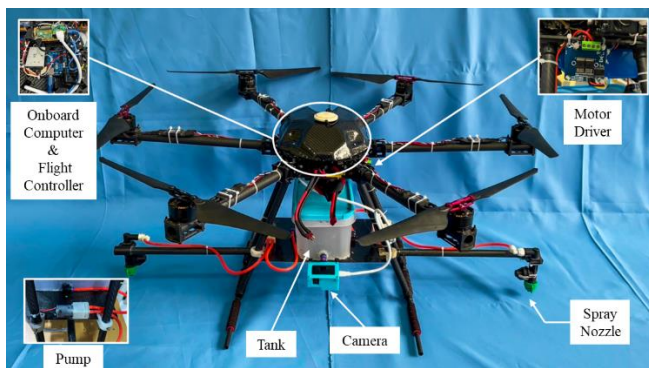

Fig. 12. An agricultural application vision-based aerial spray system shows the essential components.

The developed sprayer drone is designed to meet specific hardware requirements, ensuring optimal performance. It has a maximum take-off weight of approximately 12 kg and can carry a payload of up to 6 kg. The system's total weight, including the spray system, is 5.835 kg, making it lightweight and suitable for various applications. The equipment features a mini pump spray motor, allowing for a maximum flow rate of 800 ml per minute, promptly ensuring efficient and effective spraying.

Table II shows the hardware requirements deployed for the vision-based UAV sprayer system. The device includes a flat fan-type agricultural spray nozzle operating at an angle of 110 degrees and an onboard tank capable of carrying about 3 kilograms of a liquid solution, providing adequate capacity for covering a significant area before needing a refill. The spray nozzle comes equipped with a manually adjusted flow rate switch to ensure that both nozzles function at the same rate. A priming diaphragm mini pump spray motor allows for atomization energy of the spray dispersion, and the electrically generated pumping pressure indicates the minimum possible and

practical spray deposit. To ensure that the drone sprayer system accurately follows the planned path, an RTK GPS is integrated into the system.

The device also features an onboard computer comprising a high-resolution GoPro camera and a Raspberry Pi for handling image processing functions. These components enable the drone to execute precise and efficient spraying operations while capturing high-quality footage for post-spraying analysis. Overall, the developed sprayer drone is a robust, reliable, and versatile system suitable for a wide range of applications in agricultural settings.

TABLE II
SPECIFICATION OF THE VISION-BASED UAV SPRAYER SYSTEM
DEPLOYED IN THE STUDY

Details	Item description	Specifications
Drone frame	Frame	Carbon fiber
	Type	Hexacopter
Drone motor	Type	Brushless direct current motor
	Weight	148 grams
	Speed	320 KV
	Thrust	1860G @1660 prop and 70% Throttle
Video camera	Camera makes	GoPro 8
	Spectral bands	RGB
	Megapixel	4K
	Capture rate	60 frames per second
	Storage	S.D. card
Battery	Technology	Lithium-ion batteries
	Maximum capacity	30,000 mAh
R.C. controller	Make	HereLink
	Transmission distance	20km (FCC)
	Operating Frequency	2.4GHz ISM
	GPU	4 Core, Mali-T860
GPS	Make	H-RTK F9P (SKU 12017)
	Technology	GNSS (GPS, GLONASS)
	Weight	106g
	Data and update rate	RTK: 8Hz max
Flight controller	Make	Cube Orange (Ardupilot)
	Main chip	STM32H753
	CPU	400 Mhz ARM® Cortex®-M7
	RAM	1 MB RAM/2 M.B. Flash
	Interfaces	2x I2C, 2x CAN, 3x ADC
	Sensors	Three redundant IMUs, 2 Barometers, and 1 Magnetometer
Sprayer controller	Make	Raspberry Pi/Arduino
	Main chip	BCM2711/ATmega328P
	RAM	1GB/2KB SRAM
Motor pump	Mini motor pump	Priming Diaphragm Mini Pump Spray Motor
	Voltage	Up to 24Vdc
	Power	6Watts
	Lift	Up to 3 meters
Nozzle	Agricultural spray drone nozzle Orifice type	Manual switch anti-drift Fan-spray nozzle, 11003

B. The Characterization of the Applied Vegetation Index Results

The relationship between vegetation indices, such as RGBVI and sunlight conditions, is demonstrated in Table III. The data characterization process determined that the RGBVI values remained consistent across different vegetation cases and sunlight conditions. A one-way ANOVA analysis of variance for unequal sample sizes was conducted to determine the average RGB vegetation index between at least three groups by sunlight condition. This result indicates that varying levels of sunshine significantly influence the measurement of grassland's RGBVI over days planted; this includes cloudy, semi-cloudy, or sunny weather.

TABLE III
DATA CHARACTERIZATION OF RGBVI AT DIFFERENT
SUNLIGHT CONDITIONS AND VEGETATIONS SCENARIOS

Case		Sunlight Condition RGBVI		
Days of Plant (planting date)		Cloudy	Semi-Cloudy	Sunny
1. No vegetation	5	0.007	0.021	0.081
2. Less vegetation	10	0.122	0.124	0.134
3. More vegetation	15	0.199	0.202	0.162
4. Full vegetation	20	0.527	0.475	0.456

According to a study by Ishihara et al. 2015, the vegetation indices generally decrease as the solar zenith angle decreases (the sun is higher in the sky). This relationship is affected by the plants' growth stage and lighting conditions. However, in general, the increase or decrease of the solar zenith angle or sunlight conditions and the RGVBI were found to be affected by diffuse or direct light conditions in any growth stage.

The camera's captured frames were matched with vegetation index measurements for each instance on a particular day of the year (DOY) will obtain the required data. In other words, the RGBVI measurement is the frame's average pixel value corresponding to the area where the vegetation is present. The findings demonstrate that, for any vegetation case, the RGBVI values continuously rise from Case 1 to Case 4 and are at their highest when the sky is cloudy. The solar zenith angle decreases as the sun rises higher in the sky.

Figure 13 illustrates the mathematical models of three vegetation indices based on different environmental light conditions: cloudy, semi-cloudy, and sunny. The relationship between sunlight conditions, days of plant growth, and RGB vegetation index values can be determined through regression analysis. The findings indicate that lower vegetation index values are commonly observed during the early stages of plant growth, and sunlight conditions significantly impact these values. These results can be used to rank the relative significance of factors influencing the dependent variable, namely, RGB Vegetation Index Values. As the vegetation grows, the RGBVI value generally increases, reaching its maximum measurement when all vegetation is present. Notably, measurements under cloudy sky conditions can influence the amount and type of light present, resulting in the maximum value. Various factors, including the solar zenith angle and the amount of sunlight present, can affect the RGBVI value. The sun's angle can affect the amount and quality of light reaching the vegetation, subsequently influencing the RGBVI value. The type of sunlight present, diffuse or direct, and its intensity can also affect the RGBVI value. Therefore, for accurate measurements, careful consideration must be given to the type and amount of light available when assessing vegetation using this method.
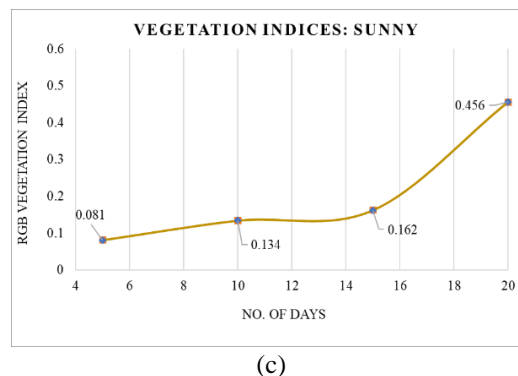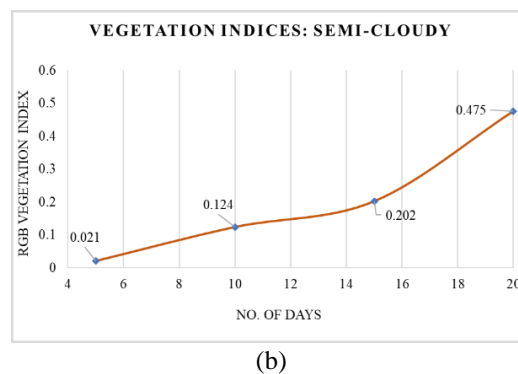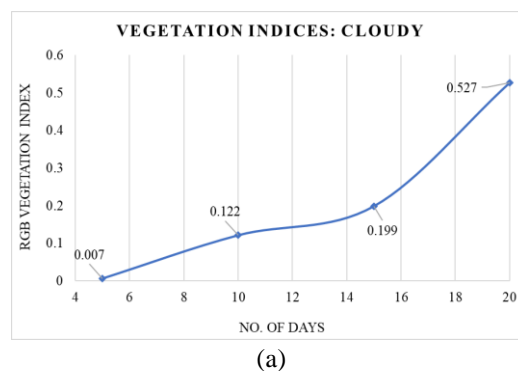
(a)

(b)

(c)

Fig. 13. RGBVI mathematical models were applied at varied sunlight conditions due to (a) cloudy, (b) semi-cloudy, and (c) sunny environments.

One factor affecting RGBVI is the solar zenith angle, which is the angle between the sun and the zenith (the point directly overhead). As the zenith angle increases, the amount of sunlight reaching the vegetation decreases, resulting in lower RGBVI values. Cloudy and semi-cloudy conditions can also lead to lower RGBVI values since less sunlight is available for photosynthesis. To account for the impact of environmental factors on RGBVI, a mathematical formula was used to calculate the average RGBVI measured at specific times of the day, considering the various sun exposures that occur throughout a given plant (DOY) day. The formula allows researchers and professionals to track vegetation growth over time precisely. Figure 14 illustrates the mathematical formula for calculating RGBVI based on the solar zenith angle and the sunlight present.

The fitted mathematical equation models, including estimated values of the equation's coefficients and the vegetation indices for various weather conditions, are summarized in the following part. This information is essential for understanding the variables that affect vegetation growth and can be applied to more precisely forecast the health of plants and their long-term growth patterns.
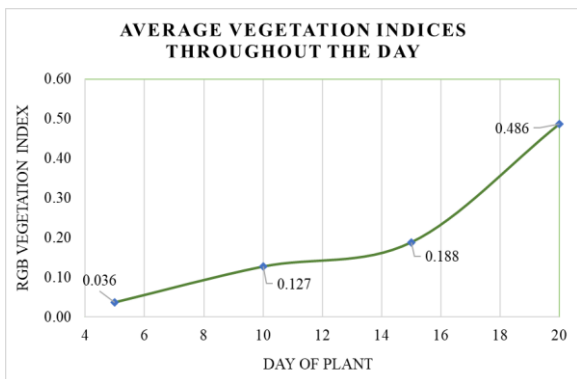
accurately represent each frame's pixel values. Refined images, such as vegetation indices, can be used for more accurate analysis. This approach offers numerous benefits, including more precise estimations of vegetation characteristics and a greater understanding of crop health and growth.

The RGBVI index for the test samples ranged from 0.0 to 0.5664, with 0.5664 being the highest possible value. Alongside the computed RGBVI, the actual plant images were compared, and it was found that when vegetation indices approach the value of 1, the plant has green leaves and is healthy. In contrast, when this value is lower, it indicates that the plants in that specific region are growing unevenly. Applying this quantitative analysis in agriculture is vital as it gives researchers and practitioners a more effective tool for monitoring plant health and growth. By measuring the RGBVI of plants in various regions, farmers can identify areas that require more attention or treatment, enabling them to optimize plant growth and productivity. The RGBVI index and analysis method offers significant benefits to the agricultural industries and will continue to play an essential role in sustainable and efficient practices in these sectors.
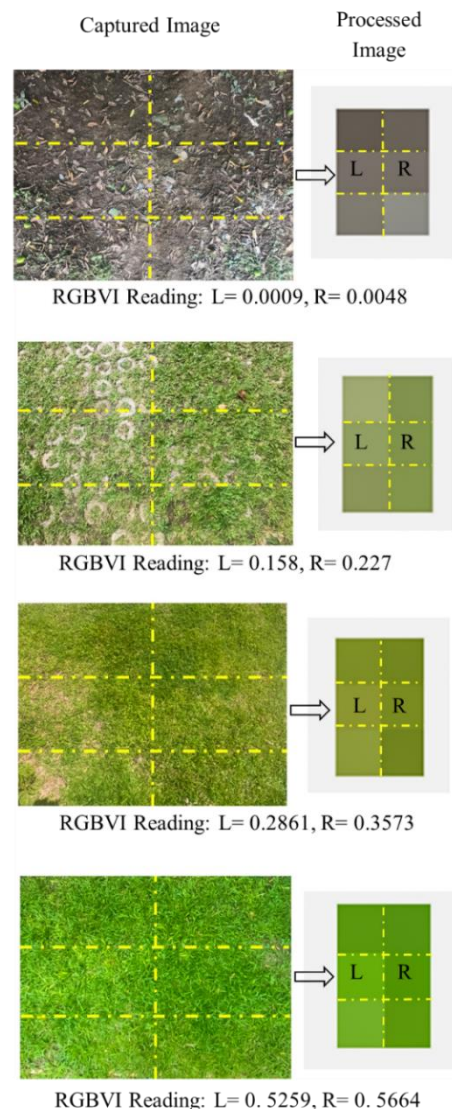

Fig. 14. Average RGBVI mathematical model at any time of day.

C. The Vision-Based Capture Image Results

Figure 15 displays a comparison of a drone-captured image with the calculated RGBVI. The RGBVI results, depicted as a pixel-like image with two columns and three rows, show the nozzle's left and right RGBVI values in the middle row. The four photos represent crop conditions ranging from poor to healthy. The vision-based RGBVI-to-PWM detection and conversion process begins by averaging out the pixel values of the frame using the video frames obtained from the GoPro camera and indicating constant dimensions as parameters.

The frames captured using the GoPro camera, combined with the designated constant dimension, serve as the parameters for averaging the pixel values of each frame. Each frame comprises red, green, and blue light mixed in varying proportions, producing a diverse range of colors on each frame. The OpenCV library features a 'simple_averaging' function to resize the image. The researchers used a two-by-three dimension to represent the red, blue, and green channels. The goal was to clearly and

Fig. 15. RGBVI values of different test samples.

D. Drone Sprayer System

The research conducted in this study aimed to optimize the spray pattern for agricultural applications. Experimental results, as illustrated in Figure 16, demonstrate that using a 100% PWM duty cycle resulted in a spray angle of approximately 72 degrees. Subsequent tests were conducted to determine the optimal spray bandwidth and minimize overlap between sprayed areas, and significant findings obtained from this evaluation are presented in Table IV. The research highlights the importance of maintaining a minimum distance of 0.9 meters between two nozzles at the determined flight height to avoid gaps and overlaps.
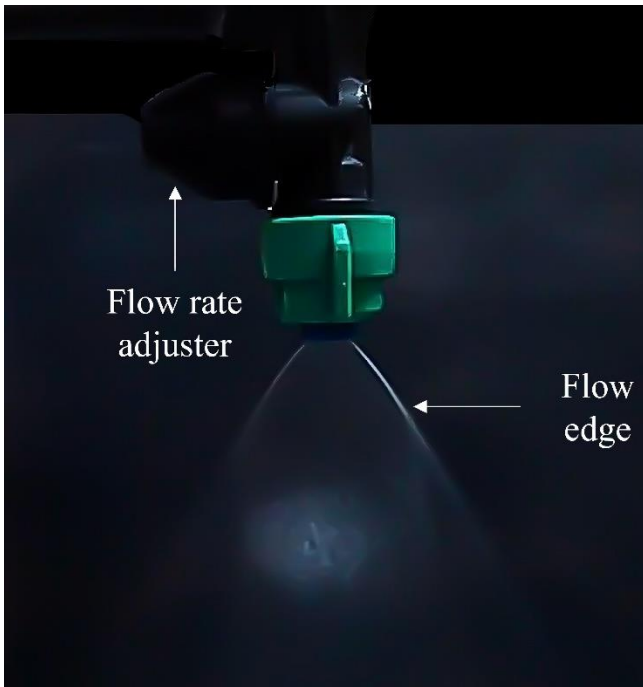

Fig. 16. Actual spray span using a 110-deg flat fan nozzle and 24 V supply voltage.

TABLE IV
SPRAY HEIGHT VS SPRAY BANDWIDTH AND GAP

Height h (m)	Spray bandwidth s (m)	Gap (m)
0.6	0.75	0.23
0.7	0.78	0.2
0.8	0.85	0.14
0.9	0.9	0.1
1.0	0.9	0.1

The performance of unmanned aerial sprayers for precise agricultural applications is crucial to ensure a significant flow rate between both nozzles, which can be achieved through calibration. This adjustment necessitates maintaining a distance of 1 meter between the nozzle's orifice and the plant tip. Figure 17 presents a flow rate comparison of two sprayers, with the PWM duty cycle set at 100% for thirty seconds at one second per cycle. The results demonstrate the effectiveness and accuracy of the calibration process, which yielded an optimal outcome and consistent performance for both sprayers. Furthermore, this evaluation showcased a strong correlation between the mini-electric motor pump and Pulse-Width Modulation (PWM) square signal duty ratio in the flow rate production of two nozzle sprayers.

The extensive testing revealed that adjusting the duty ratio can significantly impact the flow rate while maintaining accuracy and efficacy levels suitable for precision agricultural operations. With flow rates ranging from 344 to 350 mL per minute and a mere 1.73% difference in values, the consistency observed across both devices indicates an effective way to adjust sprayer performance when required. These significant findings can potentially optimize the efficiency of unmanned aerial sprayers and increase their reliability for precise agricultural applications.
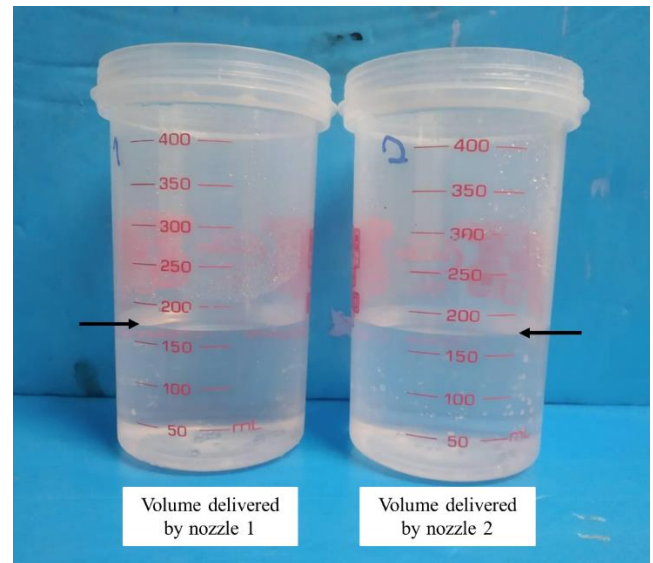

Fig. 17. Comparison of flow rate delivered by the two nozzles

The present study investigates the influence of the Pulse Width Modulation (PWM) duty cycle on spray dispersion atomization energy and its impact on spray deposit during agricultural operations. The atomization energy, essentially a function of the system flow rate and nozzle pressure, plays a vital role in droplet spreading and accelerating the spraying process. Experimental results based on droplet dispersion revealed that the square wave signal's duty cycle could be effectively controlled to manage flow rates, with the spray dispersion's atomization energy indicating the minimized possible spray deposit at a 50% PWM duty cycle. Additionally, it was found that adjusting the duty cycle period can effectively manage flow rates. It was also observed that the minimum volume deposited (V_{min}) is 2.85 mL at a 50% duty cycle period. In comparison, a 100% duty cycle resulted in a maximum volume deposited (V_{max}) of 5.78 mL over 30 seconds while performing experiments with simple spray action. Further analysis revealed an additional volume (V_{add}) of 2.93 mL, allowing for the Flow_Rate formula presented in Equation 3.

$$Flow\_Rate = V_{min} + (1 - 1.77 \times RGBVI) \times V_{add} \quad (3)$$

Experiments evaluated the relationship between two unmanned aerial sprayers' duty cycles and volumetric flow rate. By varying the duty ratio of the Pulse-Width Modulation (PWM) square signal, a correlation between the flow rate produced by the mini-electric motor pump and the duty ratio was established. Equation 5 shows a formulated mathematical representation.

In addition, the influence of the duty cycle on the flow rate was observed, enabling the optimization of the operation of the unmanned aerial sprayers.

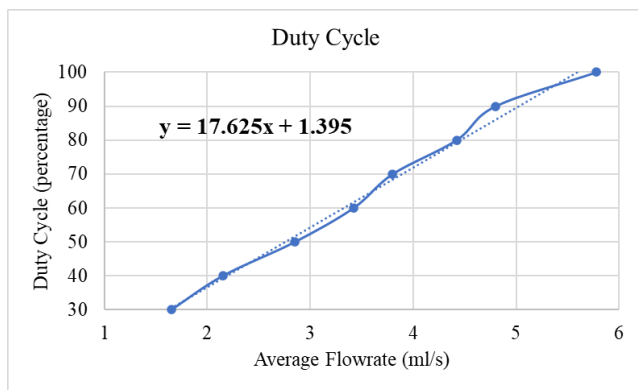$$Duty\ cycle = 17.62522 * Flow\_Rate + 1.39498 \quad (5)$$

Fig. 18. Flow volume for different duty cycles in 30-sec duration

Figure 18 shows the direct correlation between flow volume and duty cycle, obtained from measurements conducted over thirty seconds. The presented data provides valuable insights indicating that an increase in the duty cycle of the pulse-width modulation (PWM) square-wave signal leads to a corresponding augmentation in the volume of the variable system. This observation aligns with the established relationship between duty cycle and flow volume, whereby higher duty cycles result in larger volumes. The graph, accompanied by precise measurements and clear visualization, contributes to a deeper understanding of the interplay between duty cycle and flow volume in the context of the studied variable system. The findings presented in Figure 18 offer crucial implications governing flow volume modulation and facilitating more informed decision-making in designing and optimizing systems reliant on PWM control.

E. Autonomous Flight Results

The successful implementation of a vision-based unmanned aerial sprayer equipped with a variable flow rate spray system demonstrates promising potential for enhancing the efficiency and effectiveness of precision agriculture. The system underwent testing in an open field in Iligan City, Philippines, as depicted in Figure 19. During the autonomous flight, the onboard camera vision sensor processed real-time RGBVI data, while an RTK-GPS identified waypoints in an area covering

approximately 100 square meters. The system could autonomously navigate the field, providing efficient coverage for vegetable plants in the given environment while maintaining a home location 20.23 meters above mean sea level.

Using a vision-based system allowed the unmanned aerial sprayer to function autonomously, minimizing the need for human intervention and maximizing overall efficiency in drone spraying applications. This feature is critical for precision agriculture, where precision and accuracy are essential. Additionally, the variable flow rate spray system played a crucial role in enabling the precise dispensing of pesticides and fertilizers, showcasing the potential for optimal crop yields while minimizing environmental impact. Thus, precision agriculture can contribute to sustainable farming practices.

(a)

(b)

Fig. 19. (a) Actual test flight of the spray system and (b) onboard camera view for real-time RGBVI processing.

The ArduPilot Mission Planner was used to achieve autonomous flight an open-source software tool commonly utilized in unmanned aerial vehicle research. Its versatile capabilities enabled users to design custom waypoints and construct intricate flight paths, incorporating various points of interest such as loiter zones

and landing sites. The autonomous flight tests were conducted successfully, as denoted in Figure 20, demonstrating the feasibility and potential for implementing such systems in precision agriculture. Implementing an autonomous vision-based unmanned aerial sprayer with a variable flow rate spray system represents a significant innovation in precision agriculture. With its potential to increase efficiency, accuracy, and sustainability, such systems have the potential to optimize crop yields while reducing environmental impacts. Using the ArduPilot Mission Planner also highlights the potential for future advancements and the endless possibilities in unmanned aerial vehicle research.
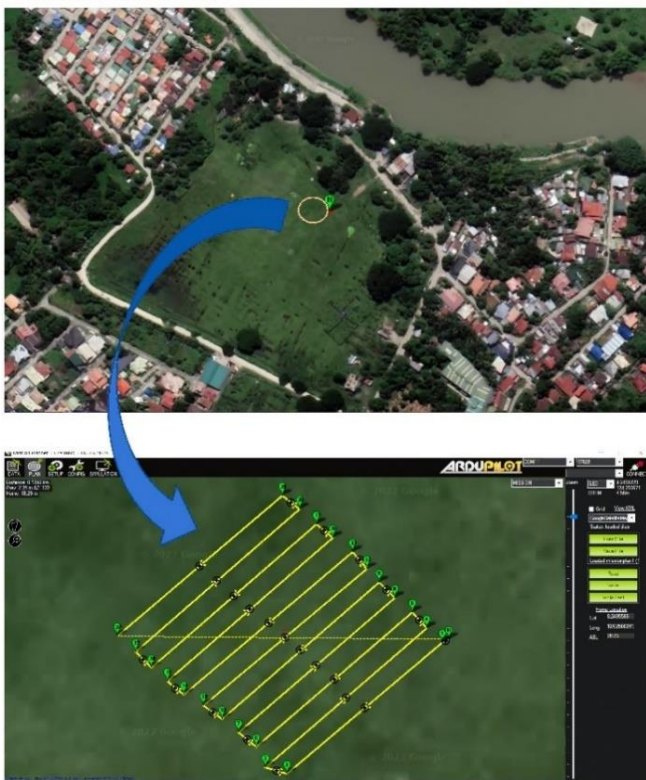

Fig. 20. Waypoints planning using the Ardupilot Mission Planner [42].

The target areas were identified and pinpointed systematically, and a flight path was established that allowed the UAV to cover them while maintaining a consistent altitude and velocity. Implementing the ArduPilot Mission Planner facilitated the planning of efficient flight paths, optimizing the coverage of the target areas, reducing flight time, and improving the accuracy of pesticide and fertilizer application. The predetermined waypoints were uploaded to the onboard autopilot system of the UAV, enabling the drone to execute the pre-arranged mission autonomously. The ArduPilot Mission Planner also provided flexibility in adjusting flight paths based on environmental conditions such as wind speed, temperature, and visibility. These considerations ensured the safe operation of the UAV within

appropriate parameters, resulting in a successful mission without disruptions. Moreover, the data collected during the flight was utilized to optimize the flight paths and ensure the accuracy of the system's application. The accuracy of the drone sprayer's planned and actual flight paths was evaluated in this study by overlaying the black line path and the dotted red line representing waypoint coordinates on recorded flight frames, as depicted in Figure 21.

The results indicated high accuracy in planned and actual flight paths, with a minimal divergence between the overlaid lines.
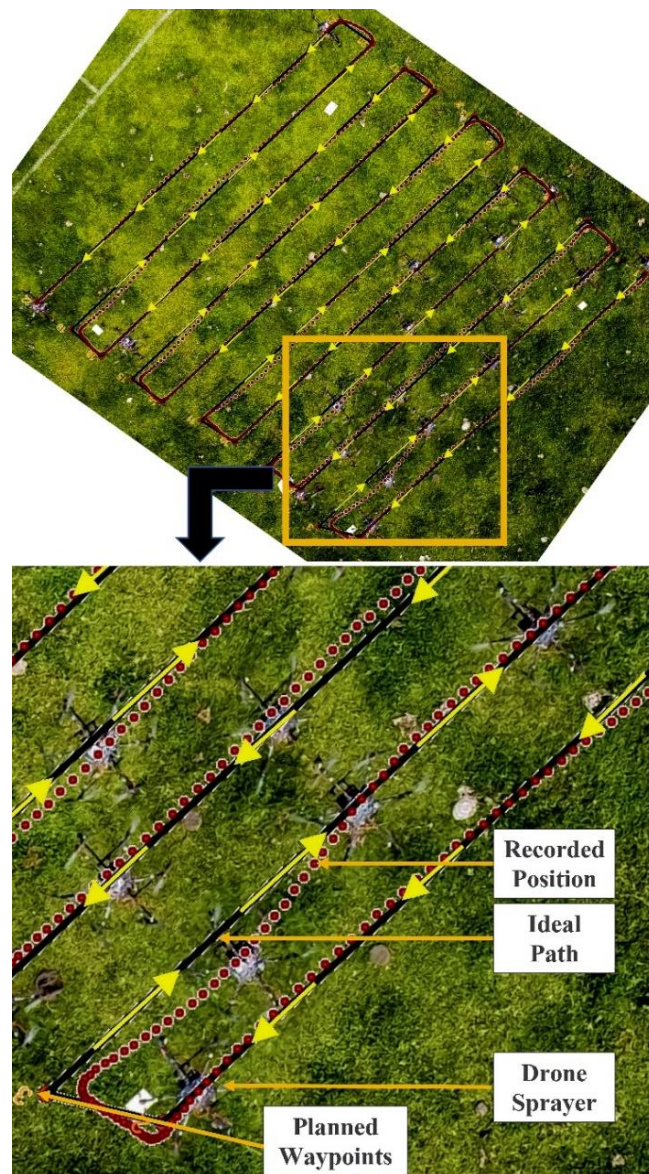

Fig. 21. Actual flight waypoints of the drone sprayer following the planned path.

Moreover, Table V provides a comprehensive understanding of the aerial sprayer system's accuracy by detailing the deviation between the intended and actual flight paths. The average deviation percentage from the planned pathway segment has been calculated considering the segment length. The results reveal that the average deviation percentage varies from 0.63% to 2.63%, with an average deviation of 1.32%. This range denotes that, on average, the

aerial sprayer system deviates from the intended path by 1.32% of the segment length. Interestingly, some pathway segments, such as 3-4, show a higher deviation percentage, while others, such as 9-10 and 17-18, have a lower deviation percentage. It is suggested that environmental factors like wind speed, altitude, or other variables may lead to these variations in deviation percentages across different segments.

<div align="center">
TABLE V
THE ACCURACY OF ALTITUDE ABOVE GROUND
</div>

Planned-Path Segment	Average Distance from Planned Pathway Segment (cm)	Deviation Percentage (%)
1-2	5.95	1.18
3-4	13.5	2.63
5-6	8.44	1.66
7-8	7.00	1.38
9-10	4.30	0.85
11-12	8.14	1.60
13-14	5.49	1.09
15-16	8.04	1.58
17-18	4.73	0.94
19-20	5.12	1.01
21-22	3.16	0.63

Furthermore, the results obtained from this study's autonomous vision-based drone sprayer indicate that the deviation between the planned and actual trajectory is stable, with an average deviation of 6.72 cm. This deviation represents approximately 1.32% of the overall distance. The stability of the deviation suggests that the system consistently adheres to the planned pathway, providing reliable and accurate coverage of the crops with a relatively small deviation.

The results indicated that the average distance between the planned pathway segment and the planned path has a relatively small deviation error percentage, as shown in Table VI. The result provided a comprehensive understanding of the aerial sprayer system's accuracy by detailing the deviation between the intended flight path and the actual path. Real-Time Kinetic (RTK) GPS technology provided precise position information in real-time, enabling the unmanned aerial sprayer to maintain accurate navigation along predetermined paths and consistent nozzle distances from crop surfaces, achieving centimeter-level precision.

The path accuracy achieved by the drone sprayer has significant implications for precision agriculture, as it allows for the precise and efficient application of pesticides and fertilizers. The results demonstrated the potential of RTK GPS technology in achieving high accuracy for unmanned aerial sprayers in precision agriculture applications. The ability to follow planned paths accurately can significantly improve the efficiency and effectiveness of crop treatments, leading to more sustainable and profitable farming practices.

The coordinates for the flight's take-off back home in terms of latitude and longitude are 8.2495565 and 124.2506241, respectively. The route design incorporates 22 waypoints spaced only 1 meter apart and has a target altitude of 5 meters. The drone sprayer installed a LiDAR sensor to keep track of the height as it was hovering above the ground. Because of the sensor, it will be possible for the drone to conform its flight path to the land's natural contours. The researchers used a second drone to record the actual flight path taken by the drone sprayer system. This drone flew over the entire waypoint region and hovered just above it. The RTK GPS makes it possible to apply precision spraying using drones, essential for achieving pinpoint accuracy in agricultural spraying applications.

<div align="center">
TABLE VI
THE AVERAGE DISTANCE FROM THE PATH PLAN
</div>

Value	Establish altitude (m)	Reported distance from LiDAR sensor (m)	Current EKF Altitude (m)
Min	5.0	4.88	4.91
Max	5.0	5.52	5.12
Average	5.0	5.205	5.016
Error	n/a	4.1%	0.2%

This study utilized an advanced LiDAR sensor to collect altitude data and facilitate precise maintenance of an average height of 5 meters above ground level while dynamically following the uneven contours of the field. The data collection approach yielded favorable results as the LiDAR sensor effectively accumulated altitude data, capturing the diverse terrain characteristics of the field under investigation with accuracy and precision, as illustrated in Figure 22. The figure comprehensively depicts the collected altitude data, visually portraying the varying elevations throughout the survey area.
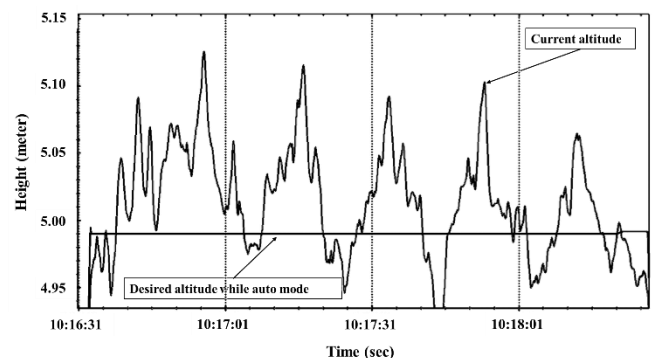

Fig. 22. LiDAR altitude, desired altitude, and current altitude

It was observed that the highest altitude recorded was 5.13 meters. The lowest was measured at 4.19 meters, confirming the sensor's ability to detect subtle elevation changes. Periodic bursts in distance readings were identified at specific turning points, namely waypoints 2-3 and 4-5, leading to transient spikes in altitude measurements. These observations can be attributed to the inherent rolling dynamics of the drone during navigation around curves, causing slight misalignments between the sensor's perpendicular orientation before entering the turns. Nevertheless, these momentary fluctuations do not significantly compromise the overall

effectiveness of the LiDAR sensor, particularly in supporting precision agriculture applications. Overall, the results highlighted the considerable potential of the LiDAR sensor as a valuable tool for capturing accurate and detailed terrain information.

The altitude control provided by the LiDAR sensor enables the consistent and efficient application of pesticides and fertilizers, even in challenging terrain. This study evaluated the accuracy of altitude control for an unmanned aerial sprayer using a LiDAR sensor and an Extra Kalman Filter (EKF) strategy. The results demonstrated that the drone could accurately maintain an altitude of 5.016 meters with a nominal error rate of just 0.02%. The low error rate indicates the remarkable precision achieved by this system, which can accurately measure altitude in even the most challenging environmental conditions due to compensation from EKF strategies employed with LiDAR sensors.

In addition, using unmanned aerial sprayers equipped with LiDAR sensors and EKF strategies has numerous advantages over traditional ground-based spraying methods. It minimizes the risk of crop damage and reduces human exposure to harmful chemicals. Furthermore, unmanned aerial sprayers' flexibility is unparalleled in their ability to perform in various conditions and terrains.

Finally, maintaining the altitude above ground demonstrates the potential for low-altitude accuracy in unmanned aerial sprayers, providing farmers with a more efficient and cost-effective method of crop protection. This improved accuracy could reduce pesticide usage, increasing sustainability and profitability within farming practices. Furthermore, these technologies can help reduce labor costs associated with manual spraying operations while improving safety by eliminating human contact with hazardous chemicals.

IV. CONCLUSIONS AND RECOMMENDATIONS

This study developed the integration of an autonomous vision-based approach to vegetation index detection into an aerial sprayer system, which would influence the variable flow rate based on the crop's health. It aimed to integrate an autonomous, vision-based vegetation index detection technique into an aerial sprayer system to enable variable flow rate control based on crop health. By incorporating an RGB camera sensor and a computer into the sprayer system, the crop's health was assessed using a simplified RGBVI calculation. The vegetation index obtained facilitated decision-making by controlling two motor pumps and regulating the variable flow rate using the PWM duty cycle approach. The aerial sprayer system, propelled by an 850-mm hexacopter with a 16-inch propeller and 320-KV brushless motor, had a maximum flow rate of 300 ml/min and a 3-kilogram liquid solution tank.

The empirical findings revealed a linear relationship between the micro-electric motor pump's flow rate and the PWM signal's duty ratio associated with the plant's RGBVI. The sprayer system effectively sprayed more agrochemicals onto plants with lower vegetative index values and less onto those with higher vegetative index values. The data indicated that an increase in the volume rate of agrochemicals corresponded to a decrease in the vegetative index value, with the highest volume rate and the lowest value observed at the highest duty cycle percentage. The onboard vision-based calculation of RGBVI demonstrated its efficacy in facilitating fluid mixtures and maximizing yield while minimizing agrochemical input.

However, it is essential to note that this investigation was limited to a 3-kg tank capacity with two nozzles operated by independent identical micromotor pumps and a spray bandwidth of flat fan nozzles captured by the camera. The study aimed to evaluate the performance of the vision-based drone sprayer in general crop applications. The results demonstrated a stable and acceptable 6.72 cm or 1.32% deviation from the intended path, falling within a reasonable range for general crop applications. The observed deviation indicates the aerial sprayer system's effective navigation and control mechanisms, ensuring accurate positioning and alignment with the intended trajectory.

Moreover, the stable and acceptable deviation from the planned pathway reduces the complexity associated with crop-specific requirements. The drone follows a specified height above the ground, maintaining a given distance using a downward-facing LIDAR provided by the ground station. When following a specified altitude above the ground, the system incurs a percentage error of 0.32%.

These findings suggest a few potential courses of action, including investigating the droplet deposits of the aerial sprayer system using a variety of nozzle types and greater drone capacity. This investigation aims to determine how the nozzle type affects the total spray coverage to the full frame captured by the vision-based plant health detection system. Through systematic exploration and optimization, we can evaluate the influence of nozzle type on spray coverage and deposition patterns. Additionally, considering the underlying physics and carefully adjusting system parameters will help maintain the desired deposition density and minimize the risk of drift. By delving into these aspects, we can improve the overall efficiency, effectiveness, and sustainability of the aerial sprayer system in agricultural applications.

REFERENCES

[1] "Palay and Corn Production in Northern Mindanao First Quarter of 2022 | Philippine Statistics Authority Region X (Northern Mindanao)," rsso10.psa.gov.ph., 2022.

[2] Magcale-Macandog, D.B., P.M.J. Paraiso, A.R. Salvacion, R.V. Estadola, S.G.L.Quinones, I.M.A. Silapan, and R.M. Briones. "An Overview of Agricultural Pollution in the Philippines: The Crops Sector." Prepared for the World Bank.Washington, D.C., 2016.

[3] M. Brankov, M. Simić, Ž. Dolijanović, M. Rajković, V. Mandić, and V. Dragičević, "The Response of Maize Lines to Foliar Fertilizing," Agriculture, vol. 10, no. 9, p. 365, Aug. 2020.

[4] M. Acharya and R. Thapa, "Remote sensing and its application in agricultural pest management," Journal of Agriculture and Environment, vol. 16, pp. 43–61, Jun. 2015.

[5] Avian Workshops, "Workshop on Drones in Agriculture- NDVI based Disease Monitoring," Tearn, 2021. http://www.tearn.academy/product/workshop-on-drones-in-agriculture-ndvi-based-disease-monitoring/ (accessed Oct. 11, 2022).

[6] M. Adan et al., "Use of earth observation satellite data to guide the implementation of integrated pest and pollinator management (IPPM) technologies in an avocado production system," Remote Sensing Applications: Society and Environment, vol. 23, p. 100566, Aug. 2021.

[7] J. Xue and B. Su, "Significant Remote Sensing Vegetation Indices: A Review of Developments and Applications," Journal of Sensors, vol. 2017, pp. 1–17, 2017.

[8] R. Ballesteros, J. F. Ortega, D. Hernández, and M. Á. Moreno,

"Characterization of Vitis vinifera L. Canopy Using Unmanned Aerial Vehicle-Based Remote Sensing and Photogrammetry Techniques," American Journal of Enology and Viticulture, vol. 66, no. 2, pp. 120–129, Jan. 2015.

[9] M. R. Adams, W. D. Philpot, and W. A. Norvell, "Yellowness index: An application of spectral second derivatives to estimate chlorosis of leaves in stressed vegetation," International Journal of Remote Sensing, vol. 20, no. 18, pp. 3663–3675, Jan. 1999.

[10] J. Lu, D. Cheng, C. Geng, Z. Zhang, Y. Xiang, and T. Hu, "Combining plant height, canopy coverage and vegetation index from UAV-based RGB images to estimate leaf nitrogen concentration of summer maize," Biosystems Engineering, vol. 202, pp. 42–54, Feb. 2021.

[11] L. Wang et al., "Vision-based adaptive variable rate spraying approach for unmanned aerial vehicles," International Journal of Agricultural and Biological Engineering, vol. 12, no. 3, pp. 18–26, 2019.

[12] S. Wang, T. Xu, and X. Li, "Development Status and Perspectives of Crop Protection Machinery and Techniques for Vegetables," Horticulturae, vol. 8, no. 2, p. 166, Feb. 2022.

[13] A. C. Watts, V. G. Ambrosia, and E. A. Hinkley, "Unmanned Aircraft Systems in Remote Sensing and Scientific Research: Classification and Considerations of Use," Remote Sensing, vol. 4, no. 6, pp. 1671–1692, Jun. 2012.

[14] K. R. Ocampo, "DA allows pesticide spraying in farms via drones," INQUIRER.net, Oct. 19, 2021, Retrieved from https://business.inquirer.net/332749/da-allows-pesticide-spraying-in-farms-via-drones.

[15] F. Ahmad et al., "Effect of operational parameters of UAV sprayer on spray deposition pattern in target and off-target zones during outer field weed control application," Computers and Electronics in Agriculture, vol. 172, p. 105350, May 2020.

[16] J. Perez, "Agriculture Drone - Everything You Need To Know," AgriBotix. 2022. Accessed: Oct. 11, 2022. [Online]. Available: https://agribotix.com/drones/

[17] Organisation for Economic Co-operation and Development (OECD), "Report on the State of the Knowledge – Literature Review on Unmanned Aerial Spray Systems in Agriculture," OECD Publishing, Paris, 2021.

[18] D. E. Martin, W. E. Woldt, and M. A. Latheef, "Effect of Application Height and Ground Speed on Spray Pattern and Droplet Spectra from Remotely Piloted Aerial Application Systems," Drones, vol. 3, no. 4, p. 83, Dec. 2019.

[19] S. Sudhakar, V. Vijayakumar, C. Sathiya Kumar, V. Priya, L. Ravi, and V. Subramaniyaswamy, "Unmanned Aerial Vehicle (UAV) based Forest Fire Detection and monitoring for reducing false alarms in forest-fires," Computer Communications, vol. 149, pp. 1–16, 2020.

[20] A. Muid et al., "Potential of UAV Application for Forest Fire Detection," Journal of Physics: Conference Series, vol. 2243, 2022.

[21] D. Erdos, A. Erdos, and S. E. Watkins, "An experimental UAV system for search and rescue challenge," IEEE Aerospace and Electronic Systems Magazine, vol. 28, no. 5, pp. 32–37, May 2013.

[22] Jeanette Pao, Carl John Salaan, Charles Alver Banglos, Karl Martin Aldueso, Lester Librado, and Jonathan Maglasang, "Shelled Drone with Meshed Net Performance Evaluation through Aerodynamic Analysis and Vibration Response Investigation," Engineering Letters, vol. 30, no.4, pp1573-1587, 2022.

[23] L. Di Puglia Pugliese, F. Guerriero, and G. Macrina, "Using drones for parcels delivery process," Procedia Manuf., vol. 42, pp. 488–497, 2020.

[24] S. Atoev, K. -R. Kwon, S. -H. Lee and K. -S. Moon, "Data analysis of the MAVLink communication protocol," 2017 International Conference on Information Science and Communications Technologies (ICISCT), Tashkent, Uzbekistan, pp. 1-3, 2017.

[25] Shinya Kawabata, Kodai Nohara, Jae Hoon Lee, Hirotatsu Suzuki, Takeaki Takiguchi, Oh Seong Park, and Shingo Okamoto, "Autonomous Flight Drone with Depth Camera for Inspection Task of Infra Structure," Lecture Notes in Engineering and Computer Science: Proceedings of The International MultiConference of Engineers and Computer Scientists 2018, 14-16 March, 2018, Hong Kong, pp804-808.

[26] Masataka Kan. Author, Shingo Okamoto, and Jae Hoon Lee, "Development of Drone Capable of Autonomous Flight Using GPS," Lecture Notes in Engineering and Computer Science: Proceedings of The International MultiConference of Engineers and Computer Scientists 2018, 14-16 March, 2018, Hong Kong, pp665-669.

[27] Ye Chen, RuHui Huang, and Yi Zhu, "A Cumulative Error Suppression Method for UAV Visual Positioning System based on Historical Visiting Information," Engineering Letters, vol. 25, no.4, pp424-430, 2017.

[28] J. Dijk, Adam, Olga Rajadell Rojas, G. J. Burghouts, and K. Schutte, "Image processing in aerial surveillance and reconnaissance: from pixels to understanding," Proc. SPIE 8897, Electro-Optical Remote Sensing, Photonic Technologies, and Applications VII; and Military Applications in Hyperspectral Imaging and High Spatial Resolution Sensing, 88970A, October 2013.

[29] M. Basso et al., "Proposal for an Embedded System Architecture Using a GNDVI Algorithm to Support UAV-Based Agrochemical Spraying," Sensors, vol. 19, no. 24, p. 5397, Dec. 2019.

[30] P. Teng et al., "Estimation of Ground Surface and Accuracy Assessments of Growth Parameters for a Sweet Potato Community in Ridge Cultivation," Remote Sensing, vol. 11, no. 12, p. 1487, Jun. 2019.

[31] Y. Liu et al., "A Robust Vegetation Index Based on Different UAV RGB Images to Estimate SPAD Values of Naked Barley Leaves," Remote Sensing, vol. 13, no. 4, p. 686, Feb. 2021.

[32] S. B. Sulistyo, W. L. Woo, and S. S. Dlay, "Regularized Neural Networks Fusion and Genetic Algorithm Based On-Field Nitrogen Status Estimation of Wheat Plants," IEEE Transactions on Industrial Informatics, vol. 13, no. 1, pp. 103–114, Feb. 2017.

[33] S. Kawashima, "An Algorithm for Estimating Chlorophyll Content in Leaves Using a Video Camera," Annals of Botany, vol. 81, no. 1, pp. 49–54, Jan. 1998.

[34] M. Pagola et al., "New method to assess barley nitrogen nutrition status based on image colour analysis: Comparison with SPAD-502," Computers and Electronics in Agriculture ,vol. 65, no. 2, pp. 213–218, Mar. 2009.

[35] M. R. Golzarian and R. A. Frick, "Classification of images of wheat, ryegrass and brome grass species at early growth stages using principal component analysis," Plant Methods, vol. 7, no. 1, p. 28, 2011.

[36] R. L. Rorie et al., "Association of 'Greenness' in Corn with Yield and Leaf Nitrogen Concentration," Agronomy Journal, vol. 103, no. 2, p. 529, 2011.

[37] C. Adhikari et al., "On-farm soil N supply and N nutrition in the rice–wheat system of Nepal and Bangladesh," Field Crops Research, vol. 64, no. 3, pp. 273–286, Dec. 1999.

[38] M. Louhaichi, M. M. Borman, and D. E. Johnson, "Spatially Located Platform and Aerial Photography for Documentation of Grazing Impacts on Wheat," Geocarto International, vol. 16, no. 1, pp. 65–70, Mar. 2001.

[39] D. M. Woebbecke, G. E. Meyer, K. Von Bargen, and D. A. Mortensen, "Color Indices for Weed Identification Under Various Soil, Residue, and Lighting Conditions," Transactions of the ASAE, vol. 38, no. 1, pp. 259–269, 1995.

[40] C. J. Tucker, "Red and photographic infrared linear combinations for monitoring vegetation," Remote Sensing of Environment, vol. 8, no. 2, pp. 127–150, May 1979.

[41] J. Bendig et al., "Combining UAV-based plant height from crop surface models, visible, and near infrared vegetation indices for biomass monitoring in barley," International Journal of Applied Earth Observation and Geoinformation, vol. 39, pp. 79–87, Jul. 2015.

[42] "Mission Planner Home — Mission Planner documentation," Ardupilot.org, 2019. http://ardupilot.org/planner/.